Available online at www.sciencedirect.com
SCIENCE DIRECT
ELSEVIER
Continental Shelf Research 24 (2004) 983–1000
CONTINENTAL SHELF RESEARCH
www.elsevier.com/locate/csr

Biogeographical regions of the tropical and subtropical Atlantic Ocean off South America: classification based on pigment (CZCS) and chlorophyll-*a* (SeaWiFS) variability

Adriana Gonzalez-Silvera[a,*], Eduardo Santamaria-del-Angel[a], Virginia M. T. Garcia[b], Carlos A.E. Garcia[c], Roberto Millán-Nuñez[a], Frank Muller-Karger[d]

[a] *Facultad de Ciencias Marinas, Universidad Autónoma de Baja California Apart.Postal 453, Ensenada, BC C.P. 22800, Mexico*
[b] *Department de Oceanografia, Fundação Universidade Federal do Rio Grande (FURG), Rio Grande, RS C.P. 474-CEP 96901-800, Brazil*
[c] *Department de Fisica, Fundação Universidade Federal do Rio Grande (FURG), Rio Grande, RS C.P. 474—CEP 96901-800, Brazil*
[d] *College of Marine Science, University of South Florida, Florida, USA*

Received 6 February 2003; received in revised form 14 January 2004; accepted 5 March 2004

Abstract

Tropical and subtropical Atlantic Ocean waters off the coasts of Brazil, Uruguay and Argentina are influenced by a variety of hydrographic processes that lead to a great diversity in the biological system. In situ observations are scarce and sparsely distributed over this zone. Phytoplankton pigment concentrations were estimated utilizing the *Coastal Zone Colour Scanner* for the area located between 5°N and 45°S, and from the coast of South America eastward to 25°W. *Advanced Very High Resolution Radiometer* (sea surface temperature) and data from literature were used to differentiate regions, considering space and time variations of the phytoplankton biomass. Monthly pigment concentration time series were used for the period of January 1982–May 1986 as input for a Principal Component Analysis (PCA). The PCA analysis grouped 152 locations into 14 regions, most of them associated to clear surface circulation patterns and hydrographic features. These results were confirmed using monthly composites of chlorophyll-*a* concentration from *Sea-viewing Wide Field-of-view Sensor* for the period September 1997–April 2002. A connection between the 1982/83 and 1997/98 ENSO events and pigment distribution over southern and southeastern Brazil, as well as the Argentinean continental shelf, was clearly evidenced in temporal pigment distributions. Results presented in this work contribute to the idea that ocean colour images are an appropriate tool to identify and follow the seasonal displacement of biogeographical region boundaries.

Keywords: CZCS; SeaWiFS; Oceanic province; Phytoplankton; Monthly distribution; Southwestern Atlantic Ocean (5°N and 45°S).

*Corresponding author. Tel.: +52-646-1744570; fax: +52-646-1744103.
E-mail addresses: agglez@uabc.mx (A. Gonzalez-Silvera), santamaria@uabc.mx (E. Santamaria-del-Angel), docvmtg@super.furg.br (V.M.T. Garcia), dfsgar@super.furg.br (C.A.E. Garcia), rmillan@uabc.mx (R. Millán-Nuñez), carib@carbon.marine.usf.edu (F. Muller-Karger).

0278-4343/$ - see front matter
doi:10.1016/j.csr.2004.03.002

1. Introduction

Assessment of global primary oceanic production is an important goal in biological oceanography today. Models of primary production based on the use of phytoplankton biomass obtained by remote sensors can be useful in addressing this problem (Platt et al., 1991; Morel, 1991; Falkowski, 1998). Several of the approaches for modelling phytoplankton primary production through remote sensing require the assumption that variables which define the shape of the vertical biomass profile (chlorophyll-*a*) and the photosynthetic parameters of the $P-I$ curve (P_m^B and α^B) are known and stable within regions and seasons (Platt et al., 1991). This led to the concept of Biogeographical Provinces (Longhurst et al., 1995), dividing the ocean into areas with distinct physical, chemical and biological features where these assumptions can be applied.

In a global approach given by Longhurst et al. (1995), waters along the Brazilian coast, from the coastline to 2000 m depth and from 5°S to approximately 40°S have been classified as a coastal province named the Brazilian Province (BRAZ). The Western Tropical Atlantic Ocean Province (north of 5°S) and the South Atlantic Gyre Province (south of 5°S) limit the BRAZ province. This division (Longhurst et al., 1995) was based on historical information of general surface circulation patterns observed in this area. However, along the continental shelf off the coasts of Brazil, Uruguay and Argentina circulation patterns are modified by topography, upwelling and continental runoff (Castro and Miranda, 1998; Piola et al., 2000). This raises the hypothesis that the biogeographical provinces proposed by Longhurst et al. (1995) can be divided into smaller regions.

The definition of biogeographical provinces and regions requires a large data set on temporal and spatial variations of phytoplankton biomass and parameters for primary production modelling. However, along the Western Atlantic Ocean and specifically off the coast of Brazil, there are few published data sets and field data are sparsely distributed (Brandini et al., 1997). A similar problem was analysed previously (Santamaria-del-Angel et al., 1994) in the Gulf of California and the authors used weekly composites of pigment concentration from Coastal Zone Colour Scanner (CZCS) and Principal Component Analysis (PCA) to divide the gulf in biogeographical regions. In this paper, data were used from remote sensors (CZCS and Advanced Very High Resolution Radiometer—AVHRR), from literature (cited herein) and the same statistical analysis in an attempt to establish a biogeographical division that takes into consideration the space and time variations of phytoplankton biomass. Finally, images from the Sea-viewing Wide Field-of-view Sensor (SeaWiFS) sensor were used for discussion and comparison with previous results. Seasonal and spatial variability of phytoplankton biomass was considered to infer similar patterns of variability on parameters for primary production models and in doing so, the classification presented will be useful for effective regional adaptations of such models.

2. Methodology

This study is based on the statistical analysis of time series from monthly compositions of pigment concentration, with 18 km of pixel resolution, obtained from the CZCS and covering the January 1982–May 1986 period. The data sets were obtained from CD-ROMs distributed by the Jet Propulsion Laboratory (JPL, CA/USA). They were processed by NASA's Goddard Space Flight Center (Esaias et al., 1986) as described by Feldman et al. (1989). In addition, fully interpolated pigment fields were computed using the "back propagation" neural-net method (Rumelhart et al., 1986).

These time series were generated from a single pixel at 152 sampling locations along the study area, located in the southwestern Atlantic ocean, 5°N to 45°S and 25°W (Fig. 1). Inshore locations had less distance between them than those offshore. This was done in order to evaluate the coastal processes better, which are more dynamic and have more variability. In order to assess spatial variations over the entire study region, median, standard deviation and minimum and

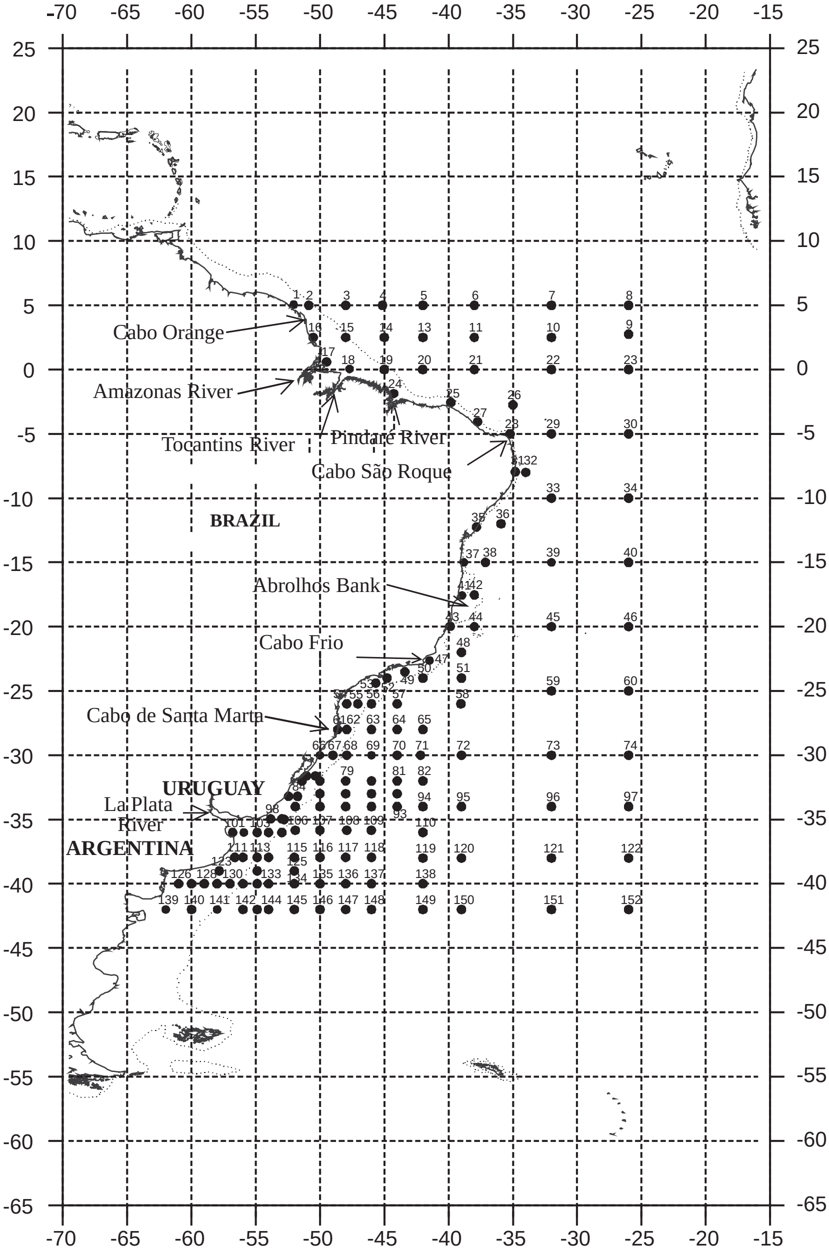

Fig. 1. Study area and location of sites where temporal series data were extracted. The dotted line indicates the 200 m isobath.

maximum pigment concentration values were calculated based on the entire time series. A PCA was applied to the data set, in order to separate discrete regions inside the study area, grouping those locations with a similar pattern of monthly variability. Thus, each location was treated as a variable ($n_v = 152$) and each month as the object describing such variable ($n_o = 53$). The matrix (152×53) was transformed into a correlation matrix (152×152) that was used as input for PCA calculations. Components that had an eigenvalue greater than 1.0 were taken as significant and locations were grouped according to the correlation matrix between PCA results and time series location. Each location was grouped with the component showing the highest correlation coefficient. In some cases, locations grouped within the same component had different sign, positive or negative, and were considered separately. Locations belonging to the same group were defined as a biogeographical region (R). A few locations that were spatially separated were classified by PCA as being part of the same group(s); however, in these cases and due to the geographic distance between them, they were considered as part of a different biogeographical region. During presentation of results each case will be discussed separately.

Monthly Sea Surface Temperature (SST) images from AVHRR for the same study period were used, both as a tool to help define the limits between biogeographical regions in some situations, and to evaluate seasonal variation inside each of them. However, they have not been inserted in PCA calculations. These images also come from the same CD-ROMs set distributed by JPL having also 18 km of pixel resolution. They belong to Multi-Channel Sea Surface Temperature (MCSST) data produced by the NOAA NESDIS MCSST retrievals, by the University of Miami, School of Marine and Atmospheric Sciences (UM/RSMAS) and by the Physical Oceanography Distributed Active Archive Center at JPL. Open areas were interpolated using an iterative Laplacian relaxation technique.

SeaWiFS monthly composites of chlorophyll-*a* concentration were used in order to confirm the results obtained with CZCS monthly composites. Images were used from September 1997 to April 2002 at 9 km of resolution. Once the classification of biogeographical regions based on CZCS was complete, time series of chlorophyll concentration were extracted using SeaWiFS data set. An area inside each identified region was chosen that comprised at least 50% of the total area of that region, and from that, average pigment concentration was calculated. These average series were considered as representative of each region. Three or four random points inside a region were chosen and each compared with the average time series in order to confirm that such average represented that biogeographical region. Using a chi-square test, the results yielded confirmed of this hypothesis with 95% of confidence. The similarity among these representative series was compared using PCA, cluster and factor analysis (Manly, 1995). This approach was used to confirm the results obtained with CZCS data set.

3. Results and discussion

When CZCS imagery was analysed, it was thought that the concentration of pigments was retrieved with an accuracy of 35% for Case I waters (chlorophyll and associated pigments determine the reflectance) and the error could be even higher when there is influence of suspended and dissolved material (coastal areas). However, as accurate pigment concentration values are not of concern, the important factor being how pigment concentrations vary with time and space for each individual month. Using this procedure, the observation of similar patterns of variability that make possible to infer that a group of locations can be classified as a biogeographical region was attempted. In general, considering the complete set of images, the effect of the Subtropical Convergence Zone (SCZ), located between 35°S and 45°S, on pigment concentration is evident (Fig. 2). Another important feature that can be easily observed is the influence of the Amazon River discharge over the continental shelf and open ocean regions of northern Brazil (above 5°S). However, in images from the austral winter (see Fig. 2 for June/July 1982, 1984 and 1986), the influence of the SCZ is sometimes lost as a result of cloud coverage on the southern part of the study area and the interpolation process affected the oligotrophic conditions that prevail in open ocean areas.

Highest pigment concentration values (greater than 0.06 mg/m^3) appear below a frontal region beginning at approximately 30°S (Fig. 3), which coincides with the northern limit of the SCZ (Castello and Möller, 1977), and also, a geographic limit between tropical and temperate zones (Lentini, 1997). The orientation of the 0.06 and

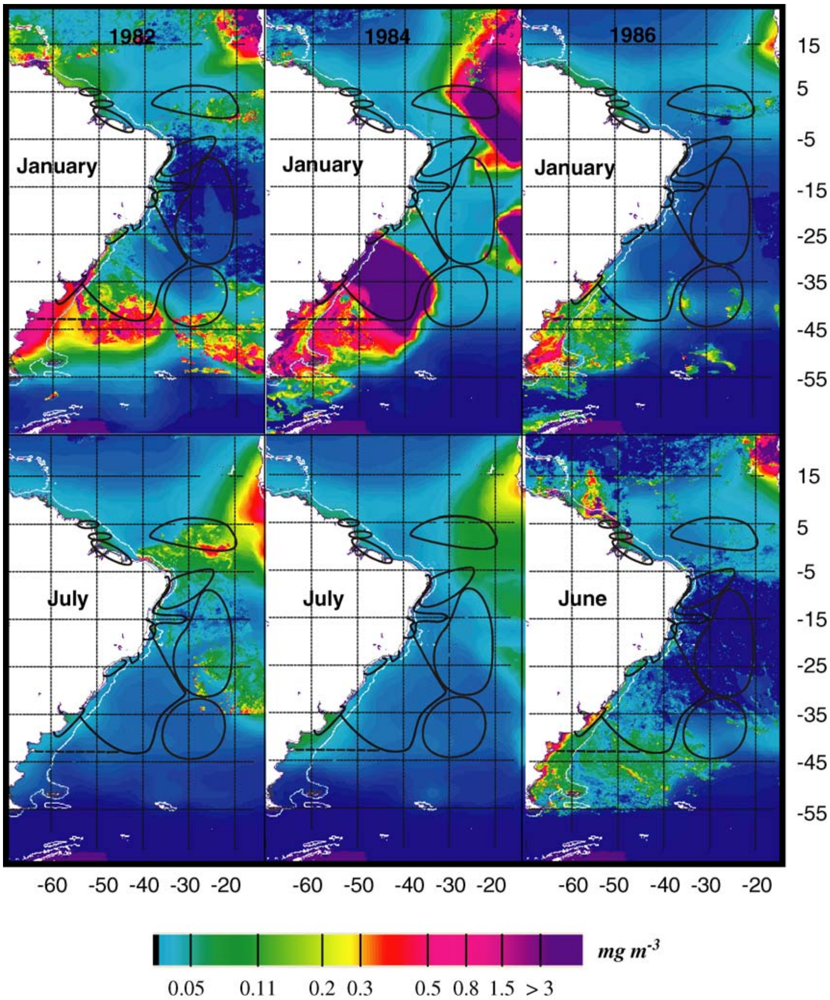

Fig. 2. Monthly composites of pigment concentration values (mg m^{-3}) from CZCS. January (austral summer) and June/July (austral winter) of 1982, 1984 and 1986. Limits of identified biogeographical regions are superimposed on images (black lines).

0.08 mg m^{-3} isolines (Fig. 3a) agrees with the average orientation of the frontal zone between Brazil and Malvinas Currents as determined by Zavialov et al. (1999). The typical front isotherm (17°C) in Zavialov et al. (1999) has a tongue-like shape, due to the southward propagation of warm Brazil Current (BC) waters along the shelf brake and this is also seen in the median distribution (Fig. 3a). Above this frontal zone there is an area with the highest maximum and standard deviation values of pigment concentrations (Fig. 3b and 3d). This area, also, shows high variability in SSTs associated to the confluence of various water masses (Garcia, 1997).

PCA analysis yielded 22 principal components (Table 1), which have been distributed in 14 biogeographical regions (Fig. 4) following the criteria described above. Table 1 summarizes these results showing the locations separated into groups and the groups separated into biogeographical regions (R). In Fig. 4, the points with the same colour comprise one group, which in general, corresponds to one region and in this case they were circled. Limits were drawn subjectively

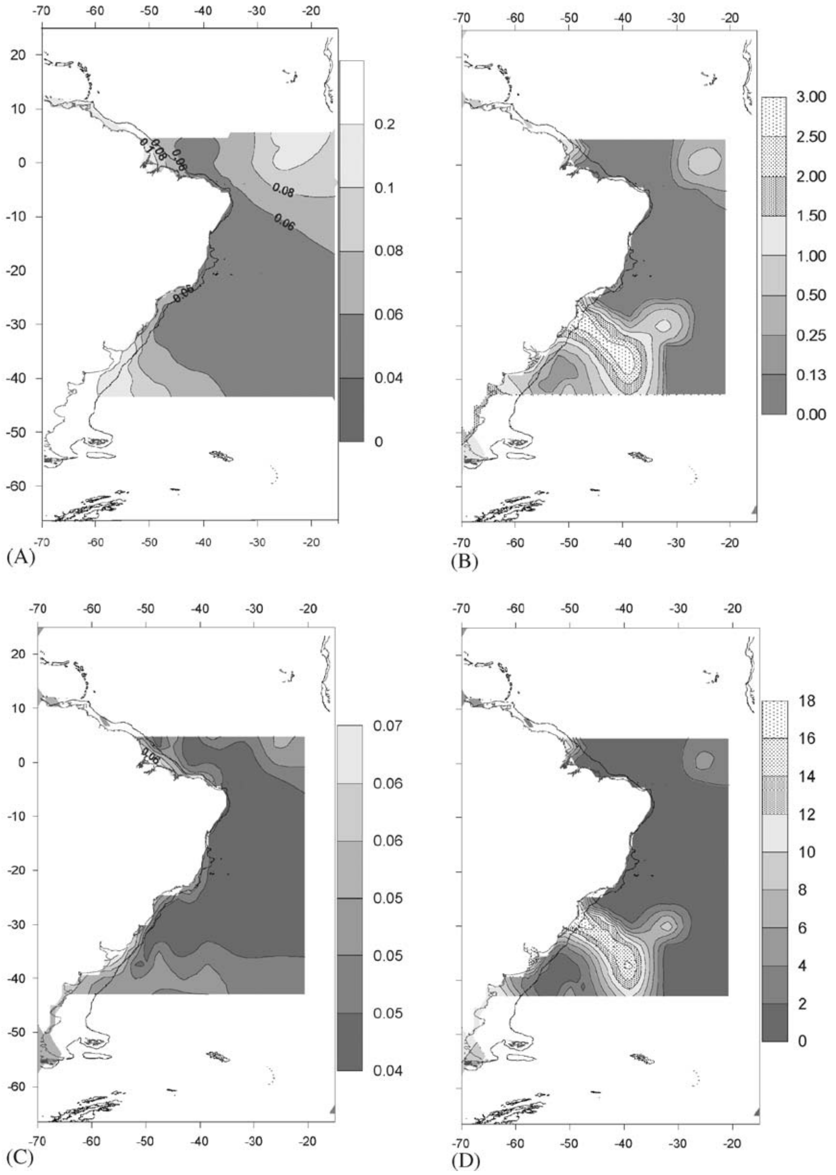

Fig. 3. Spatial distribution of median values of pigment concentration (A), standard deviation (B), minimum (C), and maximum (D) values calculated from temporal series extracted from CZCS images between January 1982 and July 1986. Values are in mg m^{-3}.

looking only for a spatial separation of locations that belong to the same region. Those limits were drawn enclosing locations, and for that reason resulting in blank spaces between them that can be considered as transitional zones. Most identified regions appear to be associated with known surface circulation patterns or hydrographic features, as summarized in Table 2. A schematic representation of the large-scale circulation patterns over the South Atlantic Ocean is presented in Fig. 5. In the section below, association with physical and/or biological features, as described in literature, with regions identified in this study was attempted.

On the northern part of our study area, regions R1, R2 and R3 are located over the northern

Table 1
Results of Principal Component Analysis, showing the components considered as significant in the analysis (PC), eigenvalue (E) and percent of variance (%) explained by each one

Comp	E	%	Group	Sampling location number and biogeographical region (bold)
PC1	57.103	0.376	1	7–8–9–10–11–23—**R4**
				34–40—**R10**
				43–44–48–51–55–56–57–61–62–63–64–65–66–67–68–69–70–71–72–73–75–76–77–78–79–80–81–82–83–84–85–86–87–88–89–90–91–92–93–94–95–99–100–105–106–107–108–109–110–116–117–118–119–120–123–136–137–138–148–149—**R11**
PC3	13.184	0.087	2	21–27
				60—**R10**
			3	47–50—**R8**
				104–112–113–114–115–124–125–126–127–128–129–130–131–132–133–134–135–139–140–141–142–143–144–145–147—**R13**
				152—**R14**
PC4	9.193	0.06	4	22–29
				52–53–54—**R9**
				150–**transition R14/R11**
PC5	6.863	0.045	5	4–13–19–20
PC6	4.586	0.03	6	49
				98—**R12**
PC8	3.925	0.026	7	97–122–151—**R14**
PC9	3.327	0.022	8	1–2—**R1**
				103—**R12**
			9	14
PC10	2.985	0.02	10	5
				15–16—**R2**
			11	45—**R10**
PC15	1.932	0.013	12	46—**R10**
PC16	1.891	0.012	13	30–32–33–36—**R5**
				59–74—**R10**
PC18	1.573	0.01	14	26
			15	146—**R13**
PC19	1.539	0.01	16	25
				41—**R7**
			17	58—**R11**
				101–103—**R12**
PC20	1.44	0.009	18	96–121—**R14**
PC21	1.282	0.008	19	6–28
				111—**R12**
PC22	1.032	0.007	20	3
				17–18–24—**R3**
			21	31–35–37–38–39–42—**R6**

Components were initially separated by group (Group) and then in biogeographical region (in Bold) for which sampling location numbers are indicated.

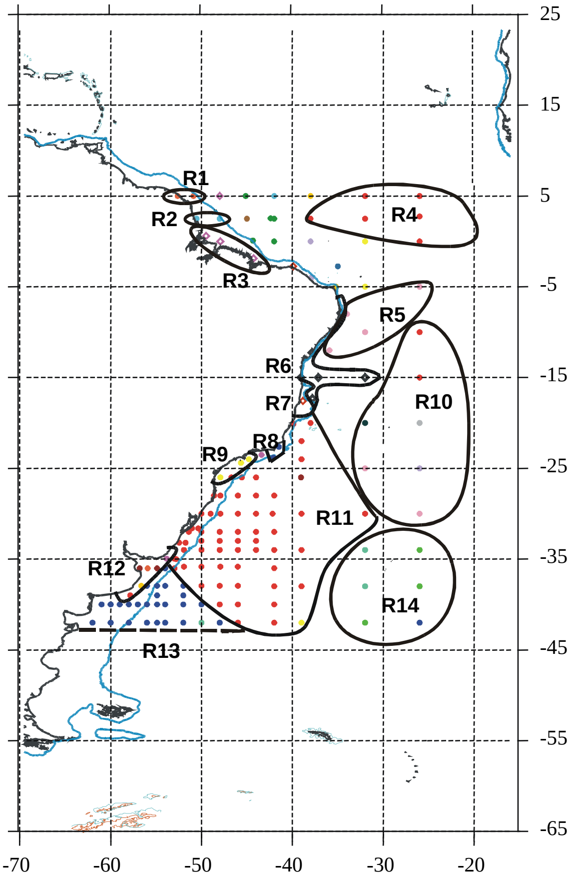

Fig. 4. Biogeographical regions (R) defined in this study. Points of same colour indicate locations belonging to the same group. Blank spaces among regions are considered as transitional zones. The blue line indicates the 200 m isobath.

Table 2
Biogeographical regions (R) identified in this study and hydrographic features associated with them

R	
1	Amazon River influence (coastal far field)
2	Amazon River influence (coastal near field)
3	Amazon River Delta
4	Western Tropical Atlantic
5	Open ocean/Northeastern Brazil
6	South Equatorial Current bifurcation
7	Abrolhos Bank (Brazil)
8	Cabo Frio upwelling region (Brazil)
9	Continental Shelf/Santos Bight (Brazil)
10	Open ocean/Subtropical Gyre
11	Brazil Current oligotrophic waters with coastal influence
12	Rio de la Plata discharge
13	Malvinas Current
14	Open ocean/subtropical front

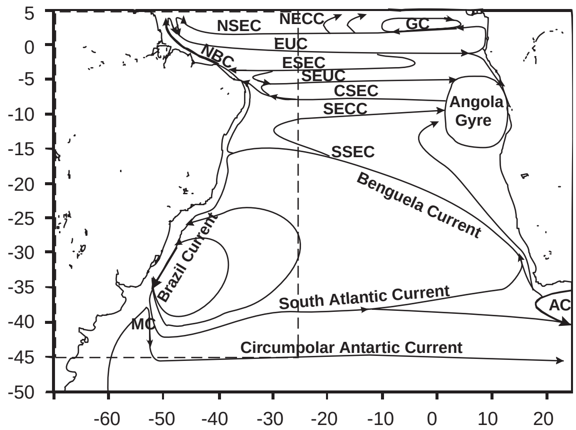

Fig. 5. Large-scale circulation for Austral fall where: Malvinas Current (MC), Brazil Current, South Atlantic Current, Circumpolar Antartic Current, Agulhas Current (AC), Benguela Current, South Equatorial Current with the northern (NSEC), equatorial (ESEC), central (CSEC), and southern (SSEC) branches, South Equatorial Countercurrent (SECC), South Equatorial Undercurrent (SEUC), Angola Gyre, Equatorial Undercurrent (EUC), North Brazil Current (NBC), North Equatorial Countercurrent (NECC), and Guinea Current (GC). The rectangle over the map (dashed line) shows the limits of the study region (adapted from Stramma and England, 1999).

Brazilian continental shelf, between 2°S and 5°N (Fig. 4). R3, which includes waters immediately off the Amazon Delta, directly influenced by the continental discharge of the Amazon, Pindaré and Tocantins rivers. The distinction between R1 and R2 is probably due to the gradual mixing of the river plume with the ocean, decreasing suspended sediment load to the northern part. Note that according to PCA analysis, the inner and outer continental shelves were not separated, in contrast to what has been shown by Geyer et al. (1996). They observed that higher chlorophyll-*a* concentrations occur in the outer shelf instead of the inner shelf due to light limitation. This is the opposite of what was observed. This simply indicates that the influence of sediment loads on CZCS measurements leads to high values of pigment concentration inshore that cannot be real. Further, it must be considered that wind conditions influence the circulation pattern of the river plume leading to seasonal differences in the size of the area covered. Under weak winds (August to October), the Amazon River plume tends to flow offshore into the open ocean as it is entrained in rings that form the retroflection of the North Brazil Current (NBC, Muller-Karger et al., 1988; Johns et al., 1990; Muller-Karger et al., 1995). This circulation pattern would explain the difference between locations 3 and 14, east of R1 and R2, respectively (Fig. 4). However, more research is required to define the conditions that lead to the boundary between R1 and R2 in this optically complex system.

Offshore, a large biogeographical region (R4) was identified comprising an area of strong variability in pigment concentration (Fig. 3), ranging from oligotrophic conditions between December and May approximately, to higher pigment levels associated with the distal end of the NBC retroflection between May and December (Muller-Karger et al., 1995). Between coastal regions (R1, R2 and R3), and the offshore region of the retroflection (R4), a large area of variable pigment concentration was identified by several components in the PCA. This area represents the centre of the NBC retroflection and is periodically affected by ring detachment. No classification has been assigned to this area in the present work, due to the changing behaviour of its pigment time series performance.

South of 5°S, R5 included four sampling locations in the open ocean (Fig. 4). These results suggest that this region has a particular behaviour with respect to the temporal variation in phytoplankton pigment concentration that should be taken in account in remote sensing of primary production. Previous works considered this zone as part of the South Atlantic Subtropical Gyre (Longhurst et al., 1995), whereas Hooker et al. (2000) left this zone without definition.

The South Equatorial Current (SEC) approaches the coast of South America between about 5°S and 15°S (Fig. 5), where it bifurcates into the NBC and the BC (Stramma and England, 1999). The NBC flows northwards over the continental shelf as a subsurface current to Cabo São Roque (5°S), where the central and equatorial branches of the SEC intensify their flux, and where they are called the intensified NBC (Schott et al., 1998). In this study, the shelf and upwelling area around 15°S has been defined as region R6, whose northern limit is also Cabo São Roque, and for this reason it is thought that there should be particular conditions that regulate phytoplankton biomass variability when considering future research.

Further south, region R7 was identified, located in the Abrolhos Bank region. This area is characterized by complex topographic features (Castro and Miranda, 1998), where BC flux slows down and turns east, altering the vertical structure of the water column and bringing up nutrients to the euphotic zone (Castro and Miranda, 1998). The influence of this hydrographic regime strongly influences phytoplankton distribution (Bonecker et al., 1993) and chlorophyll-*a* concentration (Susini-Ribeiro, 1999; Ciotti et al., 2000), defining this area as transitional, in terms of the distribution patterns of different taxonomic groups and microplankton, in relation with the low-productivity area found to the north (Gaeta et al., 1999).

The biogeographical region R8 is located at 23°S, in the Cabo Frio upwelling zone. This vigorous coastal upwelling has strong biological effects and has been associated with high primary production rates and increased fish capture (Brandini et al., 1997). Upwelling normally occurs at depths shallower than 50 m. However, when wind conditions are favourable, upwelling influence can be observed 400 km offshore, reaching southwards (Lorenzetti and Gaeta, 1996) coinciding with the area covered by R8 in this presentation.

Further south (23°S to 28°40′S) the Brazilian continental shelf has a crescent shape and this coastal orientation causes a meandering of the BC, its waters approaching the shelf edge along the bight. The inner shelf in this region is occupied by less saline waters associated with river discharges. A bottom thermal front separates inner and midshelf waters (Castro and Miranda, 1998) influencing phytoplankton biomass distribution (Aidar et al., 1993). In this study, R9 can be associated with these less saline waters, which are bounded by the oligotrophic waters of the BC offshore. This information is useful when

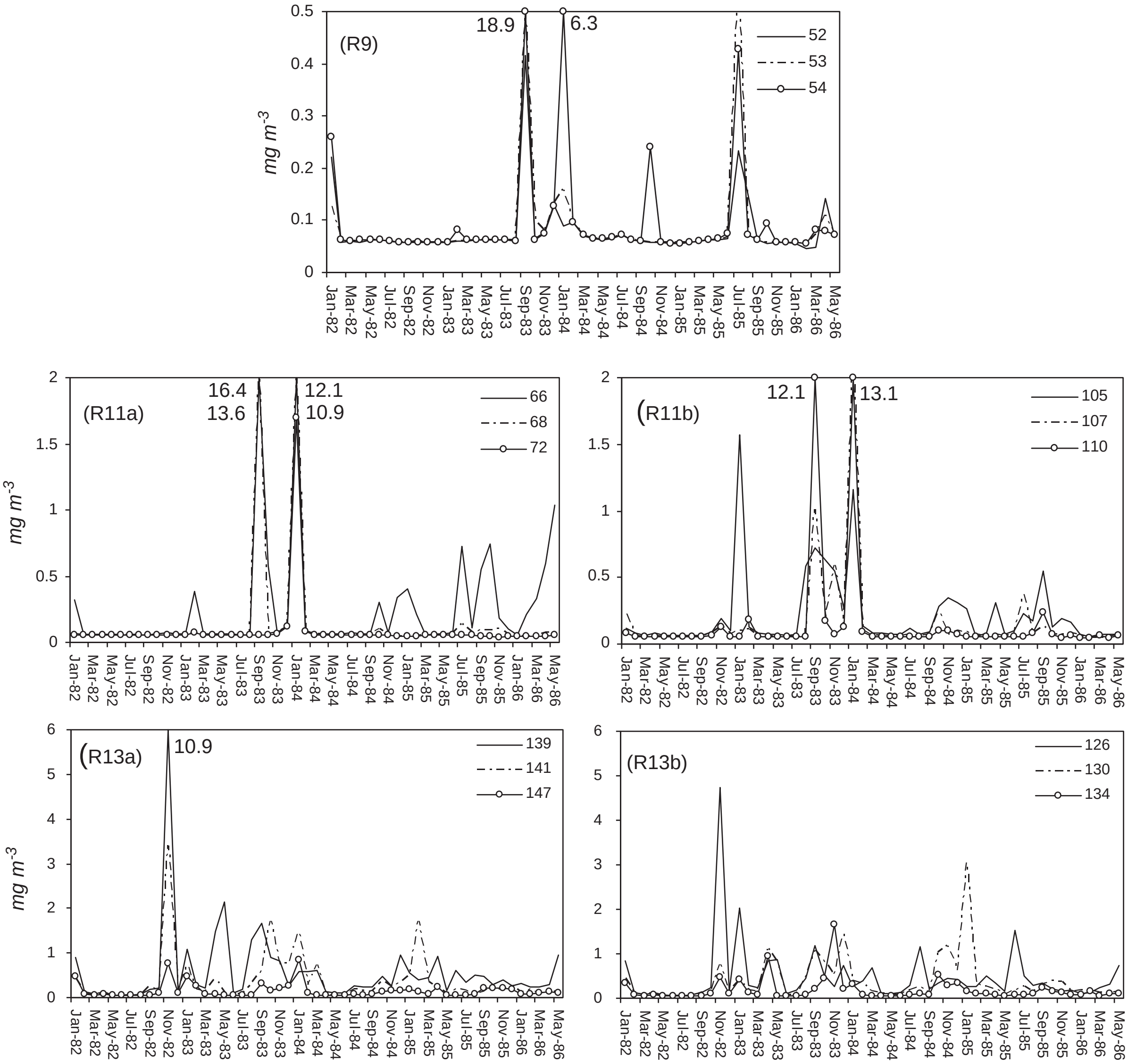

Fig. 6. Time series of pigment concentration (*Y*-axis, $mg\,m^{-3}$) extracted from CZCS images, for biogeographical regions R9, R11 and R13 (indicated on top left corner), where the 1982/83 signal is shown. Sampling location numbers are indicated on the top right corner. Values off scale are indicated.

considering the use of SST images to follow R9 limits, as tropical waters of BC are characterized by temperatures above 20°C (Emilsson, 1961). Pigment concentrations in R9 were around $0.5\,mg\,m^{-3}$ (Fig. 3), but a higher biomass signal was observed at the end of 1983 and beginning of 1984, as well as in August 1985 (Fig. 6), this will be discussed later.

Continuing southward, the southern Brazilian coast has a smoothened contour of both coastline and bottom topography (Castro and Miranda, 1998). The outer shelf is the site of convergence of two western boundary currents, the BC and the MC, forming the SCZ (Stramma and England, 1999). Less saline waters are usually found in the inner shelf due to the influence of freshwater discharge mixing with tropical waters of the BC and subantartic waters of the MC (Piola et al., 2000). The SCZ moves northward in the austral winter and southward during austral summer (Ciotti et al., 1995). At approximately 36°S, the BC completes the Subtropical South Atlantic Gyre by turning offshore (Stramma and England, 1999) and going into a recirculation cell, which turns north at approximately 30°S (see Fig. 5). The average latitude where the BC drifts from the coast (36°S) coincides with the southern limit and NW/SE orientation of region R11 in this study. Thus, this region can be associated with the oligotrophic waters of the BC and its recirculation cell. This fact can explain why R9 is separated from offshore waters while in R11 there is no separation. Previous studies in the area have shown the importance of coastal and subantartic waters in increased pigment concentration values over the continental shelf in comparison with the tropical waters of BC offshore (Ciotti et al., 1995). However, PCA results did not indicate any difference between shelf and open ocean areas. In general, pigment concentrations varied between 0.05 and $1\,\mathrm{mg\,m^{-3}}$ (Fig. 3), although higher concentrations were observed at the end of 1983 and beginning of 1984 (Fig. 6 for some locations). For that reason, it is important to consider the influence of the strong 1983/84 signal on statistic calculations (PCA), a feature that was observed in all locations that comprised this biogeographical region (Fig. 6). The interpolation process used when no data is available could be another cause for the propagation of the signal over so extensive area forcing the shelf and offshore waters to be similar. This assumption requires further investigation.

The deflection of the BC from the coast can be followed by the 21°C isotherm, whereas that of the MC is followed by the 16°C (Olson et al., 1988). In order to help investigate the seasonal variation of the SCZ over biogeographic regions of the southern section of the study area, a false colour palette was elaborated, using the whole set of AVHRR images. It can be observed, for 1983 that the 16°C isotherm moves up to Cabo de Santa Marta in winter (Fig. 7). Based on this feature, it can be proposed that R9 is limited to the south by the influence of these waters. A strong seasonal migration of both MC and BC and how this pattern extends offshore can be also observed (Fig. 7).

Region R12, between 34°S and 36°20′S, is associated with the water discharge of the La Plata River over the inner shelf and midshelf. Interaction of river and shelf waters and tidal stirring generates a turbidity front on the coast (Framiñan and Brown, 1996). This is clearly identified in satellite images as a strong gradient in reflectance and a sharp change in water colour (Gagliardini et al., 1984). For this area, several components were identified by PCA. However, it was decided to cluster them into one region, due to the marked physical and biological gradients. This was probably the cause of the heterogeneity in PCA results. Previous studies (Piola et al., 2000) indicate that the low-salinity plume ($S<33$) of La Plata River is constrained to the south of 32°S in summer, whereas it can reach 28°S in the winter, for this reason a seasonal migration of R12 limits must be considered.

Region R13 includes shelf and open ocean areas between 36°S and 42°S, following the MC and BC deflection from the coast. The inner shelf normally has less saline waters (Subantartic Shelf Waters) with highly variable stratification events (Piola et al., 2000). Our results show a strong variability in pigment concentrations in this region (Fig. 3b), with peaks at the end of 1982 (Fig. 6). However, no differences were detected between shelf and open ocean areas. This region seems to be influenced mainly by subantartic waters.

Offshore, within the tropical waters of the South Atlantic Subtropical Gyre, PCA separated locations in several components that we decided to divide into two biogeographical regions: R10, in the northern area characterized by lower pigment concentrations and R14 showed higher pigment concentrations and a stronger variability (see Fig. 3 and Fig. 4). This division was based on pigment concentration values, AVHRR images and statistical analysis. AVHRR imagery (Fig. 7) showed that while R14 is influenced by the seasonal migration of the SCZ (or Subtropical Front), R10 can be considered as part of the oligotrophic waters of the South Atlantic

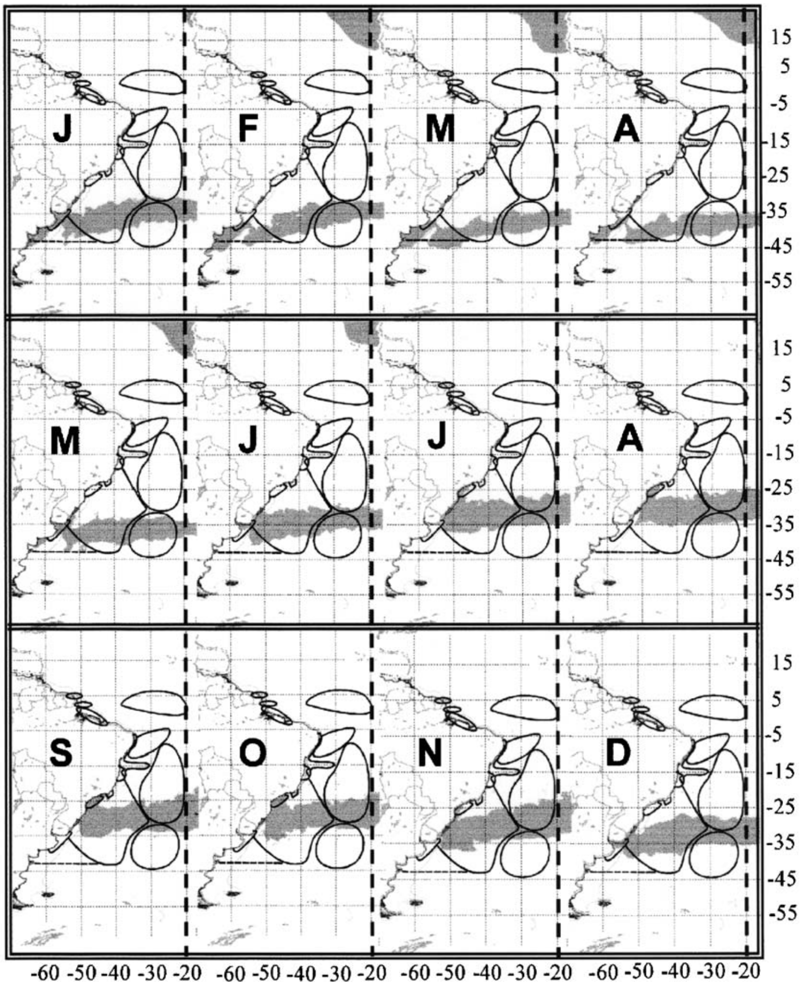

Fig. 7. SST monthly averages (AVHRR) for the period January (J)–December (D) 1983. A false colour palette was constructed to enhance the SCZ migration, where the top isoline corresponds to 21°C and the bottom isoline to 16°C. Identified biogeographical regions were superimposed.

Subtropical Gyre. In order to statistically confirm these results, a qui-square analysis was performed to test the difference between location 74 (southernmost location of R10) and locations 96 and 97 (northernmost location of R14). The difference between them was statistically significant ($p<0.001$), thus confirming separation of regions R10 and R14.

Monthly composites of chlorophyll-*a* concentration from SeaWiFS were analysed. As a first approximation, a visual examination was made of these images (from September 1997–April 2002) comparing region limits (Fig. 8). It is possible to observe the differences between austral summer (January) and austral winter (July) inside each region. It is interesting to note the winter intrusion of the NBC retroflection over the northern area between coastal regions R1 and R2, and the oceanic R4. As we have stated before, this dynamic feature causes the heterogeneity of PCA results in this area. To the south, it is important to note seasonal differences inside region R11 that present higher chlorophyll-*a* concentration in July corresponding exactly to R11 boundaries. The same can be seen for R14 that presents also higher concentrations of chlorophyll-*a* during July, according to SCZ intrusion over this zone (Fig. 7).

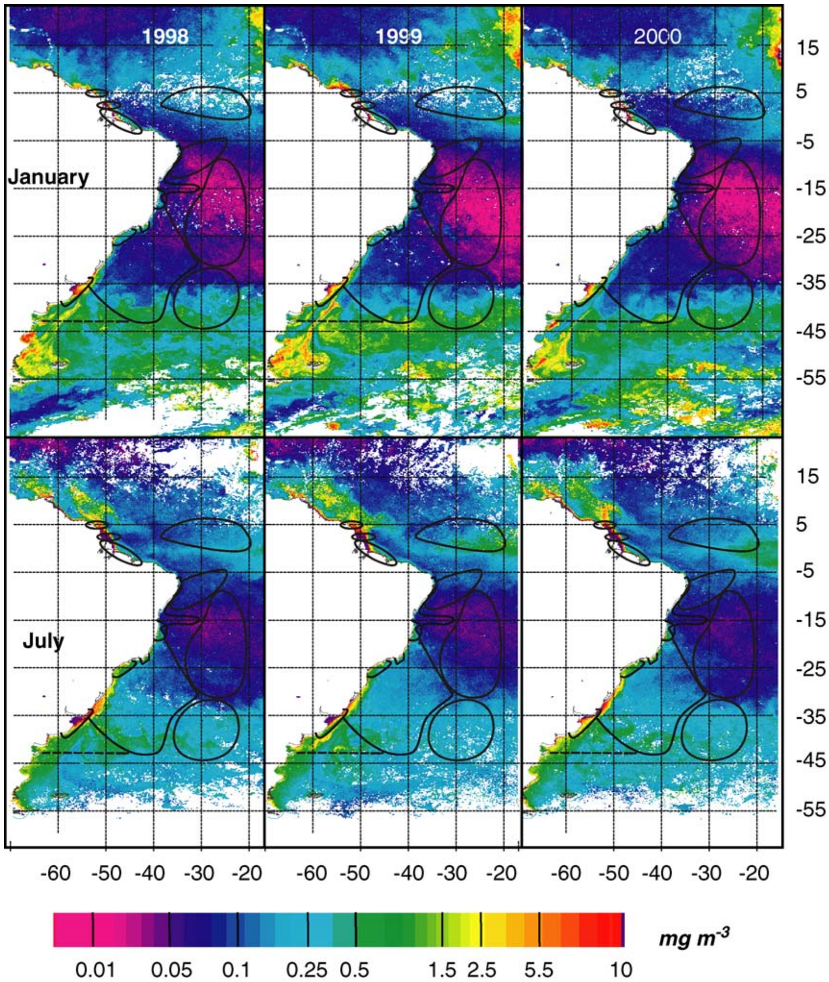

Fig. 8. Monthly composites of chlorophyll-*a* concentration (mg m^{-3}) from SeaWiFS for January (austral summer) and July (austral winter) of 1998, 1999 and 2000. Region limits are superimposed.

Representative time series of chlorophyll-*a* concentration for each region were used as input for a PCA analysis (see methodology for details), which resulted in five principal components (Table 3). R2 was grouped inside component 4 indicating its difference from the others. Regions R6 and R9 were grouped inside component 3 and although they are put together, they covariate inversely and thus they were confirmed as different regions. In component 2, regions R1 and R14 have the same pattern of inverse covariance. Most regions, however, were grouped in component 1 and all of them vary in the same manner (negative sign). A cluster analysis, using average linkage method, was applied only to those regions grouped inside component 1 and results indicate that these regions can be considered as different, although R10 and R11 are very close to each other (Fig. 9).

In order to clarify these results, a factor analysis was used with principal component as extraction method and varimax rotation (Fig. 10), which confirmed differences between variables, although R10 and R11 were found close to each other again. However, a Kruskall–Wallis analysis pointed the differences between representative series of R10 and R11 at the 95% confidence level; and the

Table 3
Results of Principal Component Analysis applied using representative series (SeaWiFS) for each biogeographical region

Region	Comp. 1	Comp. 2	Comp. 3	Comp. 4	Comp. 5
1	0.405	**−0.485**	−0.106	0.341	−0.076
2	−0.649	−0.654	0.922	**−0.935**	−0.893
3	**−0.599**	0.307	0.001	−0.024	0.075
4	**−0.231**	−0.183	0.035	−0.185	−0.156
5	**−0.636**	−0.239	0.241	−0.392	−0.393
6	−0.160	−0.117	**0.325**	−0.162	−0.114
7	**−0.571**	−0.240	0.112	−0.282	−0.328
8	**−0.349**	0.181	−0.124	−0.067	−0.005
9	−0.168	0.055	**−0.364**	0.016	0.028
10	**−0.748**	0.033	0.003	−0.316	−0.234
11	**−0.766**	0.032	−0.003	−0.317	−0.243
12	**−0.780**	−0.384	−0.079	−0.535	−0.585
13	**−0.379**	0.319	0.258	−0.257	−0.127
14	−0.261	**0.425**	0.081	−0.112	0.070

The highest correlation coefficient (in bold) indicates which region each component belongs to.

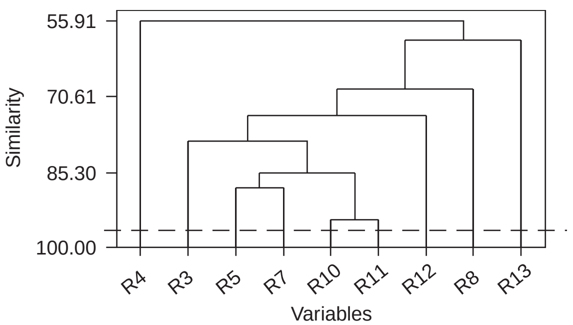

Fig. 9. Dendogram of the cluster analysis applied for representative time series obtained from SeaWiFS and corresponding to those regions grouped inside component 1 (PCA, Table 3).

similarity seen on cluster analysis can be associated with seasonal variability.

In this work we present fixed limits for biogeographical regions and it is important to consider the following: Limits between regions probably present some variability (seasonal and/or interannual) due to changes on hydrographical processes (water masses distribution). In such case, SST images (such as AVHRR) besides ocean colour images can be used to evaluate these differences. When boundaries are more related to

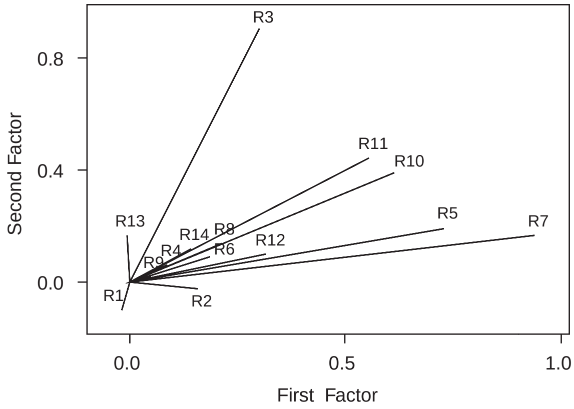

Fig. 10. Loading plot for the first and second factors from the analysis of the regions in component 1 (PCA, Table 3).

salinity, because of the importance of river discharge in those areas, in situ parameters should be measured in order to accurately determine their limits. The methodology presented by Hooker et al. (2000) to set boundaries between regions might be appropriate, because it considers changes in σ_t (which is a function of temperature and salinity), but it also requires the use of in situ data. However, if we are concerned about the use of remote sensing for primary production estimation and boundaries between regions are flexible, it would be ideal to follow these boundaries using also remote sensing. Results presented in this work contribute to the idea that ocean colour images are an appropriate tool to identify and follow the seasonal displacement of biogeographical region boundaries because they are a manifestation of vertical (upwelling) and horizontal (advection) movements of water masses and represent changes in temperature and salinity fields.

One of the strongest El Niño-Southern Oscillation (ENSO) events of this century occurred between 1982 and 1983 (Philander, 1990). Positive correlation between ENSO and high precipitation rates was previously found over the drainage basin of La Plata River (Piscioatanno et al., 1994). Negative temperature anomalies developed at 38°S and rapidly propagated northwards to approximately 25°S in spring (October to December) of 1982 (Campos et al., 1999). From the end of the summer (March) to the beginning of autumn

(April) of 1983, negative temperature anomalies were detected propagating on the opposite direction and this process was observed until December. These signals were associated with the high precipitation rates over the continental shelves of Uruguay and southern Brazil. This system was adjusted through a northward Kelvin wave that propagated over the southern and southeastern Brazilian continental shelf (Campos et al., 1999).

The effect of negative temperature anomalies in 1982/1983 can be seen in the pigment concentrations data R9, R11 and R13 (Fig. 6), indicating a strong link between phytoplankton dynamics and ENSO in these areas. In R13, the 1982 signal is obvious; time series in R11 and R9 reflect the northward anomaly propagation during 1983. However, the effect of a Kelvin wave does not explain why locations so far from the coast, as

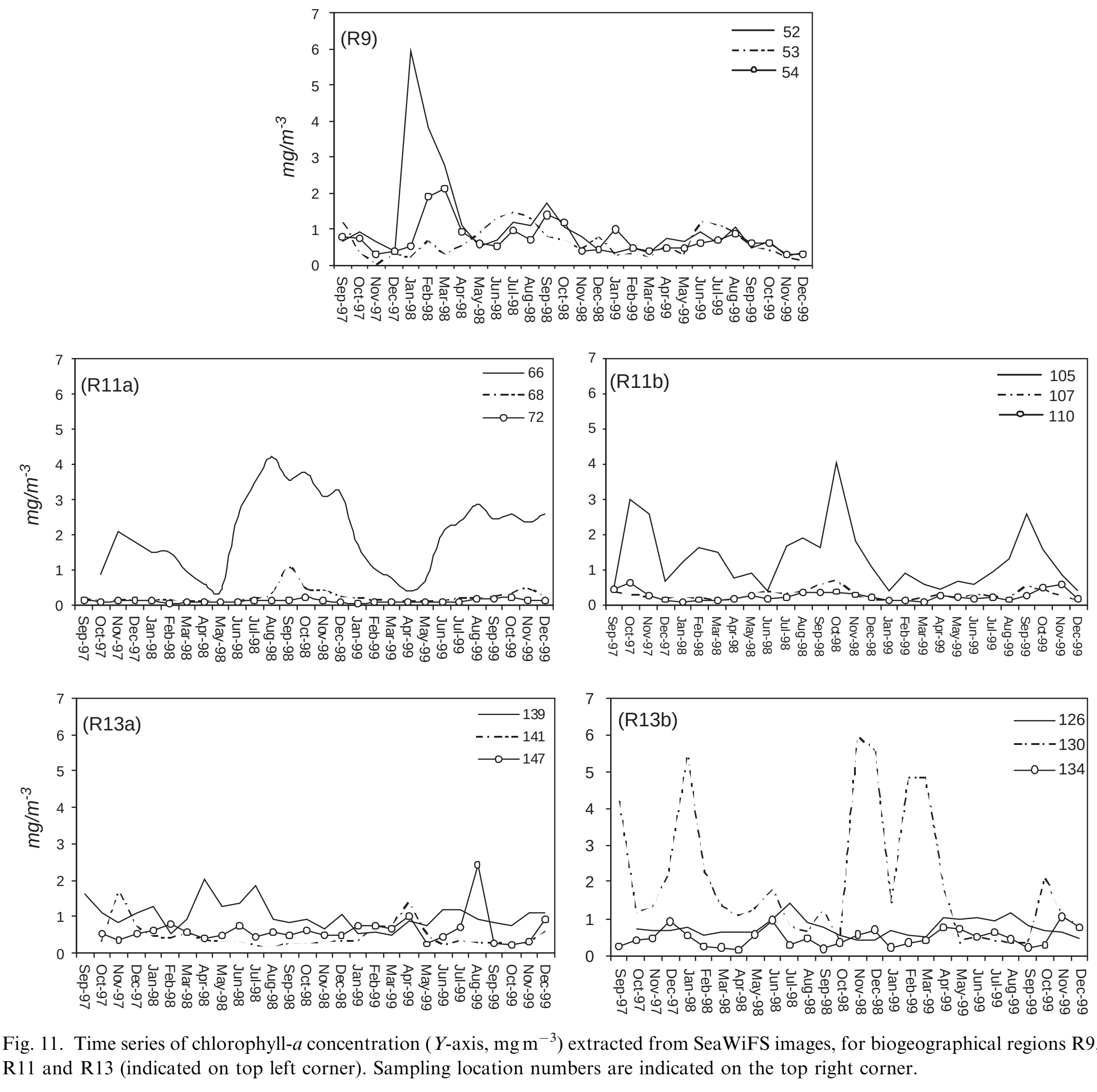

Fig. 11. Time series of chlorophyll-*a* concentration (*Y*-axis, $mg\,m^{-3}$) extracted from SeaWiFS images, for biogeographical regions R9, R11 and R13 (indicated on top left corner). Sampling location numbers are indicated on the top right corner.

those of R11, were also affected, since presumably the effect of a Kelvin wave would not be felt that far offshore (Mann and Lazier, 1991). A probable explanation could be the recirculation cell associated to the BC (Stramma and England, 1999), whose effect coincides approximately with the dimensions of this region (see Fig. 5) and might have greatly contributed to the propagation of the signal over such a large area. During 1997/1998 a new and strong El Niño event was felt worldwide. Time series of chlorophyll-*a* concentration from SeaWiFS were extracted for the same location as in Fig. 6. It is possible to observe the increase in concentrations during the end of 1997–1998 (Fig. 11). For R9 the increase was observed mainly for the southernmost location (#52) during January–March 1998. For R11 the increase in chlorophyll-*a* concentration was observed mainly during the second semester of 1998, but it is not very strong for offshore locations (#72 and 110) which could be an indication of the influence of the interpolation process on CZCS data and results presented previously. However, locations 68 and 75, in an intermediate position, have a strong signal during 1998. These results confirm the influence of El Niño on offshore areas off southern Brazil, but the exact spatial dimension of such influence will be the subject of future studies.

4. Conclusion

This study presented a description of biogeographical regions, identified by time series analyses of CZCS-derived pigment concentrations using PCA and further confirmed by statistical analysis of SeaWiFS imagery. Identified regions are related to important hydrographic patterns in the area (see Table 2) which lead to a more detailed description of provinces as was previously done (Longhurst et al., 1995; Hooker et al., 2000), particularly for coastal regions of the South Atlantic Ocean. Blank spaces between regions were a result of the location of points over the study area and a better delimitation of region boundaries is necessary in order to consider their seasonal displacement. The use of higher-resolution ocean colour images would improve precision in the definition of these areas. In addition, this work emphasizes the dynamic characteristics of biogeographical regions (and probably provinces) and the potential of ocean colour images to follow their boundaries. This fact has to be considered when employing the application of primary production models, as the necessary parameters will change inside each region or province. If an image of chlorophyll-*a* concentration is taken, regional divisions must firstly be recognized inside it, for the later application of the chosen model to calculate an image of primary production.

Acknowledgements

This work is a result of the project ''Remote Sensing of Phytoplankton Primary Production in the Southwestern Atlantic and Southern Ocean'' developed by the Ocean Colour Group of the Physical Oceanography Laboratory, Fundação Universidade Federal do Rio Grande (FURG—Brazil), in cooperation with the Universidad Autonoma de Baja California (UABC—Mexico). A.G.S. acknowledges both Conselho Nacional de Desenvolvimento Científico e Tecnológico (CNPq/Brazil) and Coordenação de Aperfeiçoamento de Nível Superior (CAPES/Brazil) for student fellowship. The authors wish to thank the revision and comments of A.M. Ciotti and an anonymous reviewer to the final manuscript.

References

Aidar, E., Gaeta, S.A., Gianesella-Galvão, S., Kutner, B., Teixeira, C., 1993. Ecossistema costeiro subtropical: nutrientes dissolvidos, fitoplâncton e clorofila-a e suas relações com as condições oceanográficas na região de Ubatuba. Sao Paulo Publicacao Especial do Instituto Oceanografico de Sao Paulo 10, 9–43.

Bonecker, S.C.L., Nogueira, C.R., Bonecker, A.T., Dias, C.O., 1993. Estudo hidrográfico e planctológico da região entre Cabo Frio (Rio de Janeiro) e Arquipéloago de Abrolhos (Bahia)—Brasil. Nerítica 1/2, 71–86.

Brandini, F.P., Lopes, R.M., Gutseit, K.S., Spach, H.L., Sassi, R., 1997. Planctologia na Plataforma Continental do Brasil—Diagnose e Revisão Bibliográfica. Technical Report REVIZEE Project, Brazil.

Campos, E.J.D., Lentini, C.A., Miller, J.L., Piola, A.R., 1999. Interannual variability of the sea surface temperature in the South Brazil Bight. Geophysical Research Letters 26, 2061–2064.

Castello, J.P., Möller, O.O., 1977. Sobre as condições oceanográficas no Rio Grande do Sul. Atlântica 2 (2), 25–100.

Castro, B.M., Miranda, L.B., 1998. Physical Oceanography of the Western Atlantic Continental Shelf located between 4°N and 34°S. In: Robinson, A.R., Brink, K.H. (Eds.), The Sea. Wiley, New York, pp. 209–251.

Ciotti, A.M., Odebrecht, C., Fillman, G., Moller, O.O., 1995. Freshwater outflow and Subtropical Convergence influence on phytoplankton biomass on the Southern Brazilian continental shelf. Continental Shelf Research 15 (14), 1737–1756.

Ciotti, A.M., Valentin, J., Silva, M.R.L.F., Lorenzetti, J.A., Garcia, V.M.T., 2000. Temporal variability of ocean color in the vicinity of Victoria–Trindade submersed sea-mounts (Brazil), Monaco, 16–20 October 2000, XV Ocean Optics Symposium, pp. 1–12.

Emilsson, I., 1961. The shelf and oceanic waters off Southern Brazil. Boletim do Instituto Oceanografico (Sao Paulo) 11 (2), 101–112.

Esaias, W.E., Feldman, G.C., McClain, C.R., Elrod, J.A., 1986. Monthly satellite-derived phytoplankton pigment distribution for the North Atlantic ocean basin. Eos Transactions AGU, pp. 67–835.

Falkowski, P.G., 1998. Using satellite data to derive primary productivity in the world ocean. In: Falkowski, P.G., Behrenfeld, M.J., Esaias, W.E., Balch, W., Campbell, J., Iverson, R.L., Kiefer, D., Morel, A., Yoder, J. (Eds.), Satellite primary productivity data and algorithm development: a science plan for mission to planet earth. SeaWiFS Technical Report Series, 42, pp. 2–17.

Feldman, G.C., Kuring, N., Esaias, W., McClain, C., Elrod, J., Maynard, N., Edres, D., Evans, R., Brown, J., Walsh, S., Carle, M., Podesta, G., 1989. Ocean color: availability of the global data set. Eos Transactions AGU, pp. 70–640.

Framiñan, M.B., Brown, O.B., 1996. Study of the Rio de la Plata turbidity front, Part I: spatial and temporal distribution. Continental Shelf Research 16 (10), 1259–1282.

Gaeta, S.A., Lorenzetti, J.A., Miranda, L.B., Susini-Ribeiro, S.M.M., Pompeu, M., De Araujo, C.E.S., 1999. The Victoria Eddy and its relation to the phytoplankton biomass and primary productivity during the austral fall of 1995. Archives of Fisheries and Marine Research 47 (2/3), 253–270.

Gagliardini, D.A., Karszenbbaum, H., Legeckis, R., Klemas, V., 1984. Application of Landsat MSS, NOAA/TIROS AVHRR, and Nimbus CZCS to study the La Plata River and its interactions with the ocean. Remote Sensing of Environment 15, 21–36.

Garcia, C.A.E., 1997. Coastal and marine environments: physical oceanography. In: Seeliger, U., Odebrecht, C., Castello, J.P. (Eds.), Subtropical Convergence Environment: The Coast and Sea in the Southwestern Atlantic. Springer, Berlin, pp. 117–121.

Geyer, W.R., Beardsley, r., Lentz, S., Candela, J., Limeburner, R., Johns, W., Castro, B., Soares, I.D., 1996. Physical Oceanography of the Amazon shelf. Continental Shelf Research 16 (5/6), 575–616.

Hooker, S.B., Rees, N., Aiken, J., 2000. An objective methodology for identifying oceanic provinces. Progress in Oceanography 45 (3–4), 313–338.

Johns, E.E., Lee, T.N., Schott, F., Zantop, R.J., Evans, R.H., 1990. The North Brazil Current retroflection: seasonal structure and eddy variability. Journal of Geophsical Research 95, 22103–22120.

Lentini, C.A.D., 1997. Estudo das variabilidades da temperatura da superfície do mar na plataforma continental sudeste da América do Sul. M.Sc. Thesis, Instituto Oceanográfico—USP, São Paulo, Brasil, 133pp.

Longhurst, A., Sathyendranath, S., Platt, T., Caverhill, C., 1995. An estimate of global primary production in the ocean from satellite radiometer data. Journal of Plankton Research 17 (6), 1245–1271.

Lorenzetti, J.A., Gaeta, S.A., 1996. The Cape Frio Upwelling effect over the South Brazil Bight northern sector shelf waters: a study using AVHRR images. International Archives of Photogrammetry and Remote Sensing 31 (B7), 448–453.

Manly, B.F.J., 1995. Multivariate Statistical Methods: A Primer, 2nd Edition. Chapman & Hall, England.

Mann, K.H., Lazier, J.R.N., 1991. Dynamics of Marine Ecosystems. Blackwell Scientific Publications, Cambridge, 466pp.

Morel, A., 1991. Light and marine photosynthesis: a spectral model with geochemical and climatological implications. Progress in Oceanography 26, 263–306.

Muller-Karger, F.E., McClain, C.R., Richardson, P.L., 1988. The dispersal of the Amazon's water. Nature 333, 56–59.

Muller-Karger, F., Richardson, P.L., McGillicuddy, D., 1995. On the offshore dispersal of the Amazon's Plume in the North Atlantic. Deep-Sea Research 42 (11/12), 2127–2137.

Olson, D.B., Podestá, G.P., Evans, R.H., Brown, O.B., 1988. Temporal variation in the separation of Brazil and Malvinas Currents. Deep-Sea Research 35 (12), 1971–1990.

Philander, S.G.H., 1990. El Niño, La Niña, and the Southern Oscillation. San Diego: Academic press.

Piola, A.R., Campos, E.D.J., Moller Jr., O.O., Charo, M., Martinez, C., 2000. Subtropical Shelf Front off eastern South America. Journal of Geophysical Research 105, 6565–6578.

Piscioatanno, G.A., Diaz, A., Cazes, G., Mechoso, C.R., 1994. El Niño-Southern Oscillation impacts on rainfall in Uruguay. Journal of Climate 7 (8), 1286–1302.

Platt, T., Caverhill, C., Sathyendranath, S., 1991. Basin-scale estimates of oceanic primary production by remote sensing: the North Atlantic. Journal of Geophysical Research 96 (C8), 15147–15159.

Rumelhart, D.E., Hinton, G.E., Wiliams, R.J., 1986. Learning Internal Representations by Error Propagation in Parallel Distributed Processing. MIT Press, Cambridge, MA, pp. 318–362 (Chapter 8).

Santamaria-del-Angel, E., Alvarez-Borrego, S., Muller-Karger, F., 1994. Gulf of California biogeographic regions based on coastal zone color scanner imagery. Journal of Geophysical Research 99 (C4), 7411–7421.

Schott, F.A., Fischer, J., Stramma, L., 1998. Transports and pathways of the upper-layer circulation in the Western Tropical Atlantic. Journal of Physical Oceanography 28, 1904–1928.

Stramma, L., England, M., 1999. On the water masses and mean circulation of the South Atlantic Ocean. Journal of Geophysical Research 104 (C9), 20863–20883.

Susini-Ribeiro, S.M.M., 1999. Biomass distribution of pico-, nano- and microplankton in the continental shelf of Abrolhos, East Brazil. Archives of Fisheries and Marine Research 47 (2/3), 253–270.

Zavialov, P.O., Wainer, I., Absy, J.M., 1999. Sea surface temperature variability off southern Brazil and Uruguay as revealed from historical data since 1854. Journal of Geophysical Research 104 (C9), 21021–21032.